

Structural Basis for Inhibition of Mutant EGFR with Lazertinib (YH25448)

David E. Heppner,^{*1,2} Florian Wittlinger,³ Tyler S. Beyett,^{4,5} Tatiana Shaurova,² Daniel A. Urul,⁶ Brian Buckley,⁷ Calvin D. Pham,¹ Ilse K. Schaeffner,^{4,5} Bo Yang,^{4,5} Blessing C. Ogboo,¹ Earl W. May,⁶ Erik M. Schaefer,⁶ Michael J. Eck,^{4,5} Stefan A. Laufer,^{3,8,9} and Pamela A. Hershberger.²

Author affiliations

¹Department of Chemistry, University at Buffalo, The State University of New York, Buffalo, NY, 14260, USA.

²Department of Pharmacology and Therapeutics, Roswell Park Comprehensive Cancer Center, Buffalo, NY, 14203, USA

³Department of Pharmaceutical and Medicinal Chemistry, Institute of Pharmaceutical Sciences, Eberhard Karls Universität Tübingen, Auf der Morgenstelle 8, 72076 Tübingen, Germany.

⁴Department of Cancer Biology, Dana-Farber Cancer Institute, Boston, MA, 02215 USA.

⁵Department of Biological Chemistry and Molecular Pharmacology, Harvard Medical School, Boston, MA, 02115 USA.

⁶AssayQuant Technologies, Inc. Marlboro, MA, 01752, USA

⁷Department of Cell Stress Biology, Roswell Park Comprehensive Cancer Center, Buffalo, NY, 14203, USA

⁸Cluster of Excellence iFIT (EXC 2180) "Image-Guided and Functionally Instructed Tumor Therapies", Eberhard Karls Universität Tübingen, 72076 Tübingen, Germany.

⁹Tübingen Center for Academic Drug Discovery & Development (TüCAD2), 72076 Tübingen, Germany

Corresponding Author

David E. Heppner

515 Natural Sciences Complex

Department of Chemistry

The State University of New York at Buffalo

Buffalo, NY 14260

Phone: (716) 645-5133

Email: davidhep@buffalo.edu

Contents

Page

Experimental Procedures	S2
X-ray Crystal Structure Data collection and refinement statistics Table S1	S6
Biochemical HTRF Table S2	S8
Supplemental Images	S9
Literature Cited	S11

Experimental Procedures

No unexpected or unusually high safety hazards were encountered in this study.

Materials

Osimertinib & Lazertinib (Selleck Chem), LN2057 made by previous methods.¹ Cells, culture supplies, and reagents. The following primary antibodies were used: pEGFR (Y1068), Cell Signaling Technology (CST) #2234S; EGFR, CST#2239S; pHER2 (Y1221/1222), CST#2243S; HER2, CST#2165S; α -Tubulin, Millipore #05-829.

Protein expression and purification

The EGFR kinase domain (residues 696-1022) and HER2 kinase domain (residues 703-1024) were cloned into pTriEx with an N-terminal 6xHis-glutathione S-transferase (GST) fusion tag followed by a TEV protease cleavage site. EGFR WT, L858R, L858R/T790M as well as HER2 was expressed after baculoviral infection in SF9 cells and EGFR(T790M/V948R) was expressed in SF21 cells. Briefly, cells were pelleted and resuspended in lysis buffer composed of 50 mM Tris pH 8.0, 500 mM NaCl, 1 mM tris(2-carboxyethyl)phosphine (TCEP), and 5% glycerol. Cells were lysed via sonication prior to ultracentrifugation at >200,000 g for 1 h. Imidazole pH 8.0 was added to the supernatant for a final concentration of 40 mM and flowed through a column containing Ni-NTA agarose beads. The resin was washed with lysis buffer supplemented with 40 mM imidazole and eluted with lysis buffer containing 200 mM imidazole. Eluted EGFR kinase domain was dialyzed overnight in the presence of 5% (w/w) TEV protease against dialysis buffer containing 50 mM Tris pH 8.0, 500 mM NaCl, 1 mM TCEP, and 5% glycerol. The cleaved protein was passed through Ni-NTA resin to remove the 6xHis-GST fusion protein and TEV prior to size exclusion chromatography on a prep-grade Superdex S200 column in 50 mM Tris pH 8.0, 500 mM NaCl, 1 mM TCEP, and 5% glycerol. Fractions containing EGFR kinase of $\geq 95\%$ purity as assessed by Coomassie-stained SDS-PAGE were concentrated to approximately 4 mg/mL as determined by Bradford assay or absorbance.

Crystallization and structure determination

WT EGFR crystals pre-incubated with 1 mM AMP-PNP and 10 mM MgCl₂ were prepared by hanging-drop vapor diffusion over a reservoir solution containing 1.0 M sodium citrate and 0.1 M MES pH = 6.5 (buffer A). EGFR(T790M/V948R) pre-incubated with 1 mM AMP-PNP and 10 mM MgCl₂ on ice was prepared by hanging-drop vapor diffusion over a reservoir solution containing 0.1 M Bis-Tris (pH = 5.5), 25% PEG-3350, and 5 mM TCEP (buffer B). Drops containing crystals in buffer B were exchanged with solutions of buffer B containing ~1.0 mM 1-5 three times for an hour and then left overnight. WT crystals were soaked with solutions of buffer A containing 1 mM lazertinib and were soaked overnight prior to harvesting. In both case, crystals were flash frozen after rapid immersion in a cryoprotectant solution with buffer A or B, for WT or T790M/V948R, respectively, containing 25% ethylene glycol. X-ray diffraction data of WT crystals was collected at 100K the Advanced Light Source a part of the Northeastern Collaborative Access Team (NE-CAT) on Beamline 24-ID-C. Data on T790M/V948R crystals or at the National Synchrotron Light Source II 17-ID-2.² Diffraction data was

processed and merged in Xia2 using aimless and dials. The structure was determined by molecular replacement with the program PHASER using the active EGFR kinase from our previous work excluding the LN2380 ligand (PDB 6VH4) for WT and similarly in the case of the inactive kinase domain from EGFR(T790M/V948R) crystals containing LN3844 (PDB 6WXN). Repeated rounds of manual refitting and crystallographic refinement were performed using COOT and Phenix. The inhibitor was modeled into the closely fitting positive $F_o - F_c$ electron density and then included in following refinement cycles. Statistics for diffraction data processing and structure refinement are shown in Table S1.

Time-dependent Kinase Inhibition Assays

Biochemical assays were performed with commercially available EGFR WT, cytoplasmic domain (669-1210), GST-tagged, Carna (Cat#/Lot#: 08-115/21CBS-0127H), EGFR [T790M/L858R], cytoplasmic domain (669-1210), GST-tagged, Carna (Cat#/Lot#: 08-510/12CBS-0765M), HER2 WT, cytoplasmic domain (679-1255), GST-tagged, BPS (Cat#/Lot#: 40230/220316-1). For reactions with EGFR proteins, reactions were performed with kinase domain enzyme concentrations of 4 nM in final solutions of 52 mM HEPES pH 7.5, 1 mM ATP, 0.5 mM TCEP, 0.011% Brij-35, 0.25% glycerol, 0.1 mg/ml BSA, 0.52 mM EGTA, 10 mM MgCl₂, 15 μ M Sox-based substrate (AQT0734). HER2 assays were conducted for osimertinib and LN2057 at 10 nM and lazertinib at 1 nM with final solutions of 52 mM HEPES, pH 7.5, 1 mM ATP, 0.5 mM TCEP, 0.011% Brij-35, 0.25% glycerol, 0.2% PEG, 0.52 mM EGTA, 20 mM MgCl₂, 15-17.5 μ M Sox-based substrate (AQT0794). Enzyme concentrations and solution conditions for HER2 assays were slightly different from EGFR kinase domains to optimize for effective time-dependent behavior for kinetic fitting as well as HER2 protein stability over the course of the activity assay. BSA was not included in this experiment to prevent interference with irreversible inhibitor characterization via off-target binding. All reactions were run for 240 minutes at 30 °C. Time-dependent fluorescence from the Sox-based substrate was monitored in PerkinElmer ProxiPlate-384 Plus, white shallow well microplates (Cat. #6008280) Biotek Synergy Neo 2 microplate reader with excitation (360 nm) and emission (485 nm) wavelengths. Inhibitors (lazertinib, osimertinib, and LN2057) were dosed between 0 and 10 μ M in 24-point curves with 1.5-fold dilutions. Fluorescence, determined with identical reactions but lacking purified enzyme or crude cell lysate was subtracted from the total fluorescence signal for each time point, with both determined in duplicate, to obtain corrected relative fluorescence units (RFU). Corrected RFU values then were plotted vs. time and the reaction velocity for the first ~40 min (initial reaction rates) were determined from the slope using GraphPad Prism (La Jolla, CA) with units of RFU/min.

HTRF Assays

Biochemical assays for EGFR and HER2 kinase domains were carried out using a homogeneous time-resolved fluorescence (HTRF) KinEASE-TK (Cisbio) assay, as described previously.³ Assays were optimized for ATP concentration of 100 μ M with enzyme concentrations WT EGFR and HER2 at 10 nM, L858R 0.1 nM, and L858R/T790M at 0.02 nM. Inhibitor compounds in DMSO were dispensed directly in 384-well plates with the D300 digital dispenser (Hewlett Packard) followed immediately

by the addition of aqueous buffered solutions using the Multidrop Combi Reagent Dispenser (Thermo Fischer). Compound IC₅₀ values were determined by 11-point inhibition curves (from 1.0 to 0.00130 μM) in triplicate. The data was graphically displayed using GraphPad Prism version 7.0, (GraphPad software). The curves were fitted using a non-linear regression model with a sigmoidal dose response.

Mass Spectrometry

Purified WT HER2 kinase domain was incubated for 2 h at room temperature with 10-fold excess Lazertinib. Proteins were denatured in 8 M urea and incubated in 10 mM TCEP for 1 h prior to cysteine carbamidomethylation with 20 mM iodoacetamide in the dark at 25°C. The TCEP concentration was brought back to 10 mM for an additional 15 min before samples were diluted to 1 M urea and subjected to proteolytic digestion with trypsin (1:50 ratio of trypsin to protein) overnight at 32 °C. Digestions were brought to 1% formic acid (FA), and peptides were dried by vacuum centrifugation and desalted over C18 zip-tip. Peptides were resuspended in 2% acetonitrile (ACN)/1% FA and analyzed by liquid chromatography-tandem mass spectrometry (LC-MS/MS) on an Ultimate 3000 RSLCnano system coupled to an Orbitrap Eclipse mass spectrometer (Thermo Scientific, Waltham, MA). Peptides were separated with a 75 min gradient of 3–48% ACN in 1% FA over an ES803A column (Thermo Scientific, Waltham, MA) and electrosprayed (spray voltage of 2.15 kV, ion transfer tube temperature 300 °C) into the mass spectrometer with an EasySpray ion source (Thermo Scientific, Waltham, MA). The following instrument parameters were used: survey scans of peptide precursors were performed at 120K FWHM resolution over an *m/z* range of 300–2,000. HCD fragmentation was performed on the top 20 most abundant precursors exhibiting a charge state from two to five at a resolving power setting of 30K and fragmentation energy of 35% in the Orbitrap. CID fragmentation was applied with 35% collision energy, and resulting fragments were detected using the normal scan rate in the ion trap. Raw data were searched against a forward and reverse human proteome (Uniprot 2011) with the HER2 (residues 703-1024) appended to it via the SEQUE⁴ST algorithm, and the following modifications were allowed: carbamidomethylation of Cys (+57.021 Da), phosphorylation of Ser/Thr/Tyr (+79.966 Da), oxidation of Met (+15.995Da) and lazertinib labeling of Cys (+ 554.276 Da). The resulting peptide hits were filtered to a false discovery rate of <1%.

Cell Experiments

H1975 lung adenocarcinoma cells were cultured in RPMI 1640 media (Corning, 1004-CV) supplemented with 10% FBS (Tissue Culture Biologicals, 35-010-CV) and 1% penicillin-streptomycin (P/S, Corning, 30-002-CI). Cells were treated with indicated TKIs at 5nM and 50nM for 2 hours. BT474 breast cancer cells were cultured in DMEM media (Gibco, 11320-033) supplemented with 10% FBS and 1% P/S. Cells were treated with indicated TKIs at 5nM and 100nM for 6 hours. Culture medium was removed, cells washed with PBS, and lysed with Triton X100/SDS lysis buffer supplemented with phosphatase inhibitor (Calbiochem, 524625) and protease inhibitor (Millipore, 539134). Protein lysate concentration was analyzed using Pierce BCA kit (ThermoFisher, 23225). Samples were resolved on pre-cast Criterion Tris-HCl protein gels (BioRad, 5671024).

Ba/F3 Cellular Antiproliferative Experiments

The parental Ba/F3 cells was a generous gift from the laboratory of Dr. David Weinstock (in 2014), Dr. Pasi Jänne (2020) and was used to generate the wildtype HER2, L858R, and L858R/T790M EGFR mutant Ba/F3 cells. These cells were previously characterized as described. All Ba/F3 cells were cultured in RPMI1640 media with 10% fetal bovine serum and 1% penicillin and streptomycin. All cell lines were tested negative for *Mycoplasma* using Mycoplasma Plus PCR Primer Set (Agilent) and were passaged and/or used for no longer than 4 weeks for all experiments. Assay reagents were purchased from MilliporeSigma (Cat# R7017-5G). Ba/F3 cells were plated and treated with increasing concentrations of inhibitors in triplicate for 72 hours. Compounds were dispensed using the Tecan D300e Digital Dispenser. Cellular growth or the inhibition of growth was assessed by resazurin viability assay. All experiments were repeated at least 3 times and values were reported as an average of n=3 with standard deviation.

Table S1. Data collection and refinement statistics.

	WT (7UKV)	T790M/V948R (7UKW)
Wavelength	0.97911	0.9793
Resolution range	46.07 - 2.401 (2.487 - 2.401)	60.56 - 2.6 (2.693 - 2.6)
Space group	I 2 3	P 1 21 1
Unit cell	145.7 145.7 145.7 90 90 90	71.0483 101.796 87.3488 90 102.367 90
Total reflections	103907 (9627)	143593 (14389)
Unique reflections	19852 (1942)	37439 (3711)
Multiplicity	5.2 (5.0)	3.8 (3.9)
Completeness (%)	98.01 (96.47)	99.74 (99.38)
Mean I/sigma(I)	10.76 (1.10)	5.96 (1.24)
Wilson B-factor	58.97	41.47
R-merge	0.08979 (1.43)	0.1658 (0.6754)
R-meas	0.1001 (1.599)	0.1914 (0.7775)
R-pim	0.04245 (0.6888)	0.0945 (0.3813)
CC1/2	0.998 (0.386)	0.983 (0.815)
CC*	0.999 (0.746)	0.996 (0.948)
Reflections used in refinement	19848 (1942)	37372 (3697)
Reflections used for R-free	998 (95)	1992 (197)
R-work	0.2107 (0.3224)	0.1945 (0.2384)

R-free	0.2433 (0.3794)	0.2501 (0.3274)
CC(work)	0.951 (0.617)	0.886 (0.815)
CC(free)	0.922 (0.105)	0.877 (0.532)
Number of non-hydrogen atoms	2380	9736
macromolecules	2297	9522
ligands	41	82
solvent	42	132
Protein residues	290	1185
RMS(bonds)	0.006	0.005
RMS(angles)	0.85	0.80
Ramachandran favored (%)	94.96	94.67
Ramachandran allowed (%)	3.24	4.56
Ramachandran outliers (%)	1.80	0.77
Rotamer outliers (%)	5.20	2.20
Clashscore	8.78	11.41
Average B-factor	66.30	44.69
macromolecules	66.30	44.72
ligands	70.35	43.68
solvent	62.17	43.08

Statistics for the highest-resolution shell are shown in parentheses.

Table S2. Biochemical activity assays (Homogenous time-resolved fluorescence HTRF) of recombinant EGFR and HER2 kinase domains. IC₅₀ values were measured from a single experiment in triplicate. The ATP concentration was 100 μM. Errors are reported as ± the standard error.

Compound	Biochemical activity IC ₅₀ (nM)			
	WT EGFR	WT HER2	L858R EGFR	L858R/T790M EGFR
Lazertinib	15±3	130±10	4.0±0.6	0.15±0.02
Osimertinib	29±7	44±9	1.0±0.1	0.58±0.08
LN2057	6.5±1 ^a	12±2	0.26±0.03 ^a	0.27±0.05 ^a

^aData from ref. Wittlinger & Heppner et al.,¹⁶

Supplemental Images.

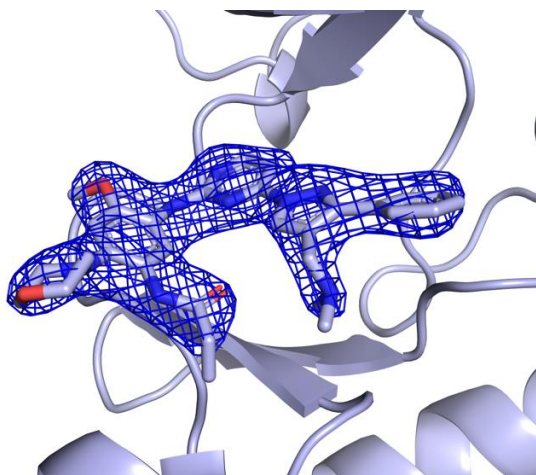


Figure S1. Positive F_o-F_c electron density map contoured at 3σ generated in PHENIX through the molecular replacement of 2.4 Å resolution data collected on WT EGFR crystals soaked with Lazertinib and coordinates of an apo WT EGFR kinase domain (PDB ID 7UKV).

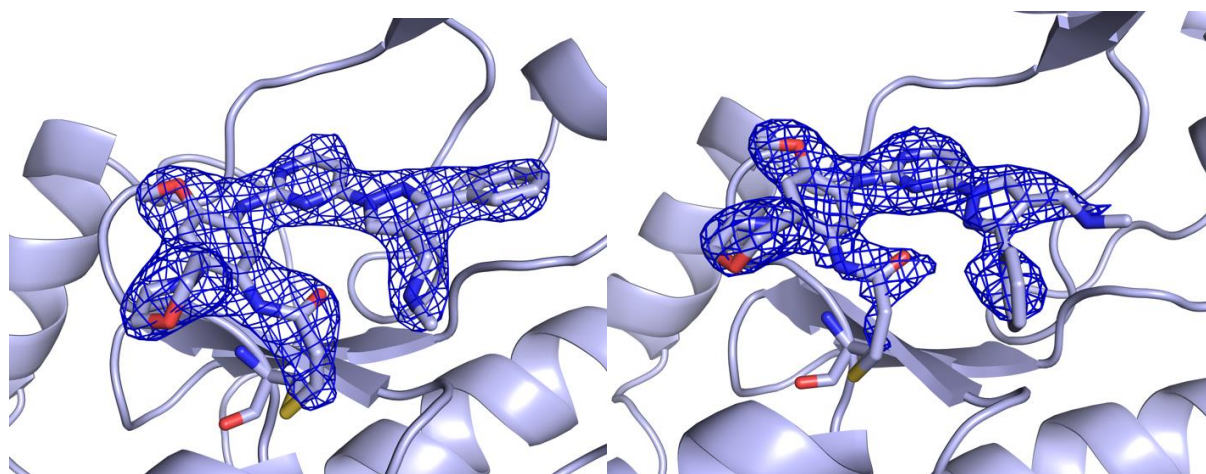


Figure S2. Positive F_o-F_c electron density map contoured at 3σ generated in PHENIX through the molecular replacement of 2.6 Å resolution data collected on EGFR(T790M/V948R) crystals soaked with Lazertinib and coordinates of a EGFR(T790M/V948R) kinase domain. Image on the left corresponds to Lazertinib bound to Chain B and right corresponds to Lazertinib in the “flipped” conformation bound to Chain A (PDB ID 7UKW).

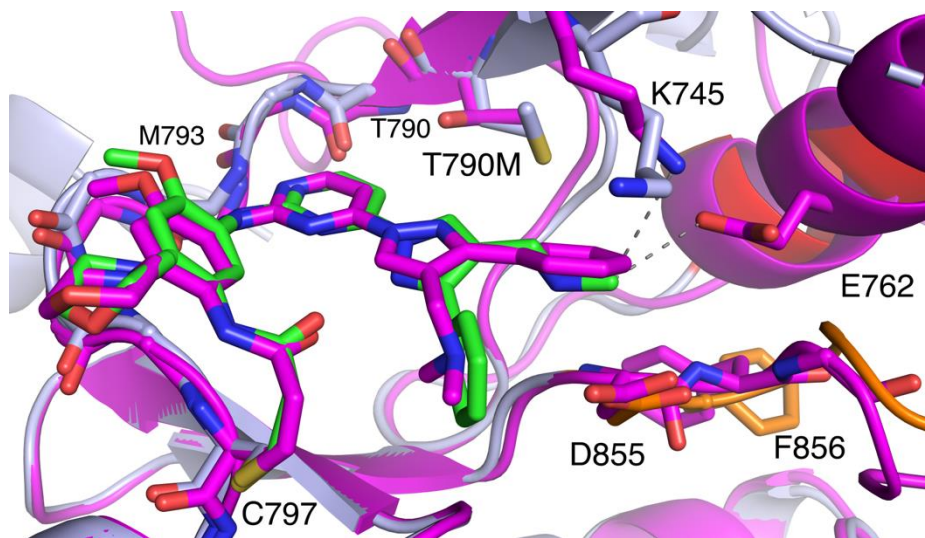


Figure S3. Structural overlay of the binding modes of WT (7VKU; magenta) and T790M/V948R EGFR (7VKW, green).

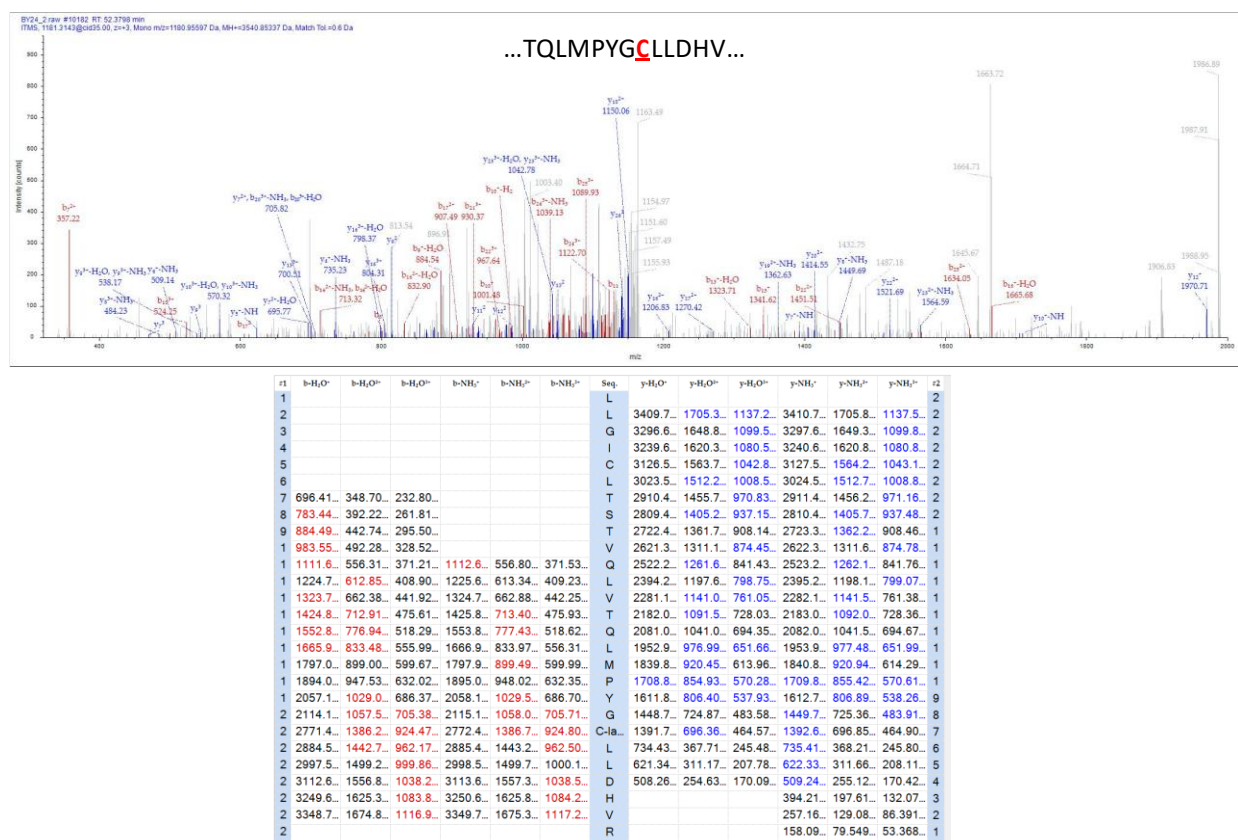


Figure S4. HER2 was digested with trypsin following labeling with Lazertinib and subjected to LC-MS/MS analysis. Top) The tryptic peptide containing C805 was identified with the mass addition +554.276 Da and labeling of C805 was confirmed by fragment ions in the MS² spectrum. Bottom) Observed fragment ion masses are tabulated alongside expected m/z values.

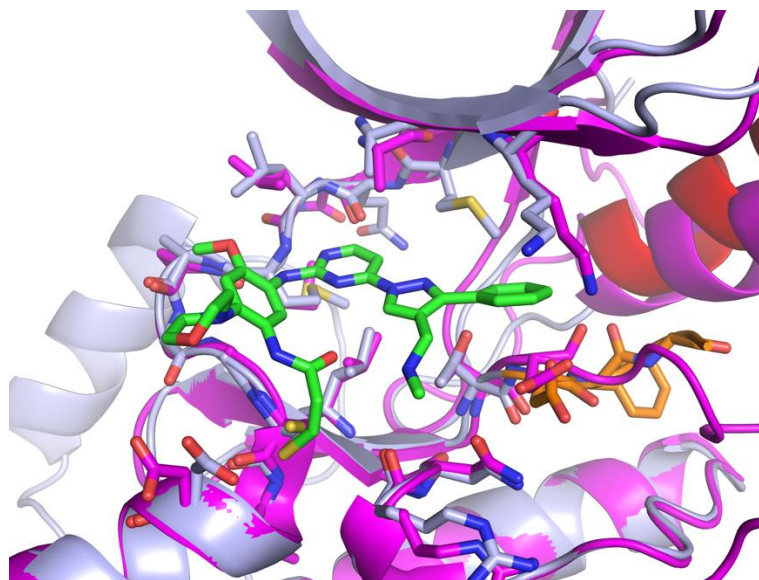


Figure S5. Structural overlay of the binding modes of lazertinib bound to EGFR(T790M/V948R) (7VKWI light blue) and WT HER2 (PDB ID 7JXK).

Literature Cited

1. Günther, M.; Juchum, M.; Kelter, G.; Fiebig, H.; Laufer, S., Lung Cancer: EGFR Inhibitors with Low Nanomolar Activity against a Therapy-Resistant L858R/T790M/C797S Mutant. *Angewandte Chemie International Edition* **2016**, *55* (36), 10890-10894.
2. Schneider, D. K.; Shi, W.; Andi, B.; Jakoncic, J.; Gao, Y.; Bhogadi, D. K.; Myers, S. F.; Martins, B.; Skinner, J. M.; Aishima, J.; Qian, K.; Bernstein, H. J.; Lazo, E. O.; Langdon, T.; Lara, J.; Shea-McCarthy, G.; Idir, M.; Huang, L.; Chubar, O.; Sweet, R. M.; Berman, L. E.; McSweeney, S.; Fuchs, M. R., FMX - the Frontier Microfocusing Macromolecular Crystallography Beamline at the National Synchrotron Light Source II. *Journal of Synchrotron Radiation* **2021**, *28* (2), 650-665.
3. Hong, L.; Quinn, C. M.; Jia, Y., Evaluating the utility of the HTRF® Transcreeener™ ADP assay technology: A comparison with the standard HTRF assay technology. *Analytical biochemistry* **2009**, *391* (1), 31-38.
4. Wittlinger, F.; Heppner, D. E.; To, C.; Günther, M.; Shin, B. H.; Rana, J. K.; Schmoker, A. M.; Beyett, T. S.; Berger, L. M.; Berger, B.-T.; Bauer, N.; Vasta, J. D.; Corona, C. R.; Robers, M. B.; Knapp, S.; Jänne, P. A.; Eck, M. J.; Laufer, S. A., Design of a “Two-in-One” Mutant-Selective Epidermal Growth Factor Receptor Inhibitor That Spans the Orthosteric and Allosteric Sites. *Journal of Medicinal Chemistry* **2022**, *65* (2), 1370-1383.